Analysis of $\mathcal{B}(\bar{B} \rightarrow X_s \gamma)$ at Next-to-Next-to-Leading Order with a Cut on Photon Energy

Thomas Becher[1] and Matthias Neubert[2,3]

[1]*Fermi National Accelerator Laboratory, P.O. Box 500, Batavia, Illinois 60510, USA*

[2]*Institute for High-Energy Phenomenology, Laboratory for Elementary-Particle Physics, Cornell University,*
Ithaca, New York 14853, USA

[3]*Institut für Physik (ThEP), Johannes Gutenberg-Universität, D-55099 Mainz, Germany*

By combining a recent estimate of the total $\bar{B} \rightarrow X_s \gamma$ branching fraction at $O(\alpha_s^2)$ with a detailed analysis of the effects of a cut $E_\gamma \geq 1.6$ GeV on photon energy, a prediction for the partial $\bar{B} \rightarrow X_s \gamma$ branching fraction at next-to-next-to-leading order in renormalization-group improved perturbation theory is obtained, in which contributions from all relevant scales are factorized. The result $\mathcal{B}(\bar{B} \rightarrow X_s \gamma) = (2.98 \pm 0.26) \times 10^{-4}$ is about 1.4σ lower than the experimental world average. This opens a window for significant new physics contributions in rare radiative B decays.

Introduction.—The inclusive decay $\bar{B} \rightarrow X_s \gamma$ is an important example of a flavor-changing neutral current process, which has been used to test the flavor sector of the standard model. Many groups have worked on improving the theoretical analysis of this process so as to keep pace with refinements in the measurements of its branching fraction. The effective weak Hamiltonian at next-to-next-to-leading order (NNLO) has been obtained by calculating multiloop matching coefficients and anomalous dimensions [1–4]. While the fermionic NNLO corrections to the $b \rightarrow s\gamma$ matrix elements have been known for some time [5], complete NNLO corrections are presently available only for the electromagnetic dipole operator [6,7]. However, an approximate result for the NNLO charm-penguin contributions has just been published [8]. Combining these ingredients, a first estimate of the $\bar{B} \rightarrow X_s \gamma$ branching ratio at NNLO has been presented in [8,9].

A complication in the analysis arises from the fact that measurements of the $\bar{B} \rightarrow X_s \gamma$ branching fraction impose stringent cuts on photon energy (defined in the B-meson rest frame), $E_\gamma > E_0$, with E_0 in the range between 1.8 to 2.0 GeV. The standard treatment is to extrapolate different measurements to a common reference point $E_0 = 1.6$ GeV using phenomenological models [10]. In that way, the experimental world average $\mathcal{B}(\bar{B} \rightarrow X_s \gamma) = (3.55 \pm 0.24^{+0.09}_{-0.10} \pm 0.03) \times 10^{-4}$ has been derived [11]. The first error combines statistical and systematic uncertainties, the second one is due to the extrapolation from high E_0 to the reference value, and the last error accounts for the subtraction of $\bar{B} \rightarrow X_d \gamma$ background. A theoretical result for the branching ratio with a cut at $E_0 = 1.6$ GeV has been derived in [8,9] using two-loop calculations of the photon-energy spectrum in fixed-order perturbation theory [12,13]. It has been argued that the extrapolation from the total to the partial branching fraction does not introduce additional theoretical uncertainties. This assertion is questionable because of the dynamical relevance of a soft scale $\Delta = m_b - 2E_0 \approx 1.4$ GeV, whose value is significantly lower than the b-quark mass.

Accounting for the photon-energy cut properly requires one to disentangle contributions associated with the hard scale $\mu_h \sim m_b$, the soft scale $\mu_0 \sim \Delta$, and an intermediate scale $\mu_i \sim \sqrt{m_b \Delta}$ set by the typical final-state hadronic invariant mass. When the cut value E_0 is chosen sufficiently low, renormalization-group (RG) improved perturbation theory can be employed to calculate the effects of the photon-energy cut using a multiscale operator product expansion [14]. In the process, logarithms of the ratio Δ/m_b are resummed to all orders. More importantly, this approach allows us to isolate the contributions associated with the lowest scale Δ, which become nonperturbative if the cut E_0 is chosen too high. We have recently performed a systematic analysis of the cut effects at NNLO. Two-loop corrections at the soft scale were calculated in [15], while those at the intermediate scale were computed in [16]. Here, the analysis is completed by extracting the two-loop hard matching corrections from a comparison with fixed-order calculations of the photon spectrum [12,13].

Using this method, we compute the fraction of all $\bar{B} \rightarrow X_s \gamma$ events with $E_\gamma \geq 1.6$ GeV with a perturbative precision of 5%. At this level of accuracy several other, nonperturbative effects need to be evaluated carefully. The event fraction receives hadronic power corrections $\sim (\Lambda_{\rm QCD}/\Delta)^n$ governed by B-meson matrix elements of local operators. The leading correction ($n = 2$) is known and turns out to be small, but terms with $n \geq 3$ are presently unknown. Recently, a new class of enhanced, nonlocal $\Lambda_{\rm QCD}/m_b$ corrections to the $\bar{B} \rightarrow X_s \gamma$ decay rate has been identified [17]. A model analysis indicates that they can affect the total decay rate at the level of a few percent.

Combining our result for the event fraction with the prediction for the total branching fraction from [8,9], we obtain

$$\mathcal{B}(\bar{B} \rightarrow X_s \gamma) = (2.98 \pm 0.26) \times 10^{-4} \qquad (1)$$

for $E_0 = 1.6$ GeV, where we have added in quadrature the uncertainties from higher-order perturbative effects

($^{+4}_{-6}$%), hadronic power corrections (5%), parametric dependencies (4%), and the interpolation in the charm-quark mass (3%). Two-loop perturbative corrections at the intermediate and soft scales significantly lower the branching fraction with regard to the fixed-order result, and they increase the theoretical uncertainty.

Scale separation and resummation.—At leading power in $\Lambda_{\mathrm{QCD}}/m_b$, the $\bar{B} \to X_s \gamma$ decay rate with a cut on photon energy obeys the factorization formula [18]

$$\Gamma(E_0) = \frac{G_F^2 \alpha}{32\pi^4}|V_{tb}V_{ts}^*|^2 \bar{m}_b^2(\mu)|H_\gamma(\mu)|^2 \int_0^\Delta dp_+(m_b - p_+)^3$$

$$\times \int_0^{p_+} d\omega\, m_b J(m_b(p_+ - \omega), \mu)S(\omega, \mu), \qquad (2)$$

where $p_+ = m_b - 2E_\gamma$ and $\Delta = m_b - 2E_0$. The function H_γ contains hard quantum corrections, the jet function J describes the physics of the hadronic final-state jet, and the shape function S parametrizes bound-state effects inside the B meson [19]. In the region of interest to our analysis, in which the quantity $\Delta \approx 1.4$ GeV can be treated as a perturbative scale, the double convolution integral in (2) can be evaluated using short-distance methods [14]. To isolate the effect of the photon cut, we focus on the fraction

of all $\bar{B} \to X_s \gamma$ events that pass the cut $E_\gamma \geq E_0$, defined as $F(E_0) = \Gamma(E_0)/\Gamma(0)$. Because the total decay rate can be computed in fixed-order perturbation theory at the hard scale μ_h, the event fraction obeys a factorization formula of the same form as (2), but with a different hard function h in place of $|H_\gamma|^2$.

Contributions associated with different mass scales can be separated from each other by evolving the various objects in the factorization formula away from a common renormalization scale μ to different "matching scales," where they can be calculated reliably using fixed-order perturbation theory. In this process, single and double logarithms of ratios of the different scales are resummed to all orders. The matching scales should be taken close to the default values $\mu_h = m_b$ for H_γ, $\mu_i = \sqrt{m_b\Delta}$ for J, and $\mu_0 = \Delta$ for S. An elegant expression describing the RG evolution of the jet function was derived in [20]. It involves an associated jet function $\tilde{j}$, which is related to J by a Laplace transform. The same technique can be applied to describe the evolution of the shape function in terms of an associated soft function $\tilde{s}$. Inserting these results into (2), the integrations over p_+ and ω can be performed, leading to

$$F(E_0) = U(\mu_h, \mu_i, \mu_0; \mu)\left(\frac{m_b}{\mu_h}\right)^{-2a_\Gamma(\mu_h,\mu)}\left(\frac{m_b\Delta}{\mu_i^2}\right)^{2a_\Gamma(\mu_i,\mu)}\left(\frac{\Delta}{\mu_0}\right)^{-2a_\Gamma(\mu_0,\mu)} h\left(\frac{m_b}{\mu_h}\right)\tilde{j}\left(\ln\frac{m_b\Delta}{\mu_i^2} + \partial_\eta\right)$$

$$\times \tilde{s}\left(\ln\frac{\Delta}{\mu_0} + \partial_\eta\right)\frac{e^{-\gamma_E\eta}}{\Gamma(1+\eta)}\left[p_3\left(\frac{\Delta}{m_b}\right) - \frac{\eta(1-\eta)}{6}\frac{\mu_\pi^2}{\Delta^2} + \dots\right] + \delta F(E_0), \qquad (3)$$

where $\eta = 2a_\Gamma(\mu_i, \mu_0) > 0$. Despite appearance, this result is independent of the choice of μ and of the three matching scales μ_h, μ_i, and μ_0. For the special case $\mu = \mu_i$, relation (3) coincides with a formula derived previously in [21]. The terms in the first line arise from the RG resummation of single and double logarithms. The precise form of the evolution factor U will be given in [22]. The exponent

$$a_\Gamma(\mu_1, \mu_2) = \int_{\mu_1}^{\mu_2} \frac{d\mu}{\mu} \Gamma_{\mathrm{cusp}}(\alpha_s(\mu)) \qquad (4)$$

is an integral over the cusp anomalous dimension. The functions h, $\tilde{j}$, and $\tilde{s}$ in the second line contain the matching corrections at the hard, intermediate, and soft scales, respectively. The two-loop expression for the jet function $\tilde{j}$ has been obtained in [16], while the two-loop result for the soft function $\tilde{s}$ can be deduced from [15]. In the argument of these functions, ∂_η means a derivative with respect to the quantity η. The hard function can be derived by matching (3) with the fixed-order expression for the photon spectrum derived in [12,13]. At the default scale $\mu_h = m_b$, we find

$$h(1) = 1 + \frac{C_F\alpha_s}{4\pi}\left[-\frac{52}{3} + \frac{7\pi^2}{6} - \sum_{i \leq j}\mathrm{Re}\frac{C_i^*C_j}{|C_7|^2}\hat{f}_{ij}(1)\right]$$

$$+ C_F\left(\frac{\alpha_s}{4\pi}\right)^2[C_F H_F + C_A H_A + T_F n_f H_f], \qquad (5)$$

where the term with $i = j = 7$ is to be excluded from the sum. The one-loop result agrees with [14], and the two-loop coefficients are given by

$$H_F = \frac{2297}{24} - \frac{229\pi^2}{18} + \frac{89\pi^4}{360} - 22\zeta_3 + 16S_a,$$

$$H_A = -\frac{50521}{648} + \frac{1259\pi^2}{108} - \frac{5\pi^4}{18} + \frac{313}{9}\zeta_3 + 16S_{\mathrm{na}}, \quad (6)$$

$$H_f = \frac{9365}{162} - \frac{19\pi^2}{27} - \frac{92}{9}\zeta_3.$$

The constants $S_a \approx 1.216$ and $S_{\mathrm{na}} \approx -4.795$ have been obtained by numerical integration in [12]. The complete expression for $h(m_b/\mu_h)$ including scale dependence will be given in [22].

In the second line of (3), the hadronic quantity μ_π^2 parametrizes the B-meson matrix element of the kinetic operator in heavy-quark effective theory. The ellipses represent unknown hadronic power corrections of order $(\Lambda_{\mathrm{QCD}}/\Delta)^3$. The polynomial

$$p_3(\delta) = 1 - \frac{3\delta\eta}{1+\eta} + \frac{3\delta^2\eta}{2+\eta} - \frac{\delta^3\eta}{3+\eta} \qquad (7)$$

derives from the $(m_b - p_+)^3$ prefactor in (2). The term $\delta F(E_0)$ in (3) collects terms that are power suppressed in the ratio $\delta = \Delta/m_b \approx 0.3$. These corrections are known in fixed-order perturbation theory, but no resummation is available. We express them as a perturbative series in powers of $\alpha_s(\mu)$. The one-loop result for δF has been given in [14], while the dominant two-loop contribution has recently been calculated in [12,13]. For subleading contributions from other operators in the effective Hamiltonian only the fermionic two-loop corrections are known [23]; they have a negligible impact on our results.

Results and conclusions.—In (3), the parameters m_b and μ_π^2 are defined in the on-shell scheme. To improve the perturbative behavior, one should eliminate them in favor of appropriately defined short-distance quantities. We use the "shape-function scheme" proposed in [24], in which low-scale subtracted heavy-quark parameters are defined via the moments of the renormalized B-meson shape function, regularized with a hard cutoff μ_f. The two-loop relations between the shape-function and pole-scheme parameters have been derived in [25]. We adopt the conventional choice $\mu_f = 1.5$ GeV and use the values $m_b = 4.61 \pm 0.06$ GeV and $\mu_\pi^2 = 0.15 \pm 0.07$ GeV^2 extracted from a fit to moments of inclusive B-decay spectra [21].

References [8,9] do not provide a result for the total $\bar{B} \to X_s\gamma$ branching fraction. The most inclusive quantity considered is the partial branching fraction defined with a mild cut at $E_0 = 1$ GeV. To combine this prediction with our RG-improved result for the event fraction, we define the ratio $T = F(1.6 \text{ GeV})/F(1.0 \text{ GeV})$. We evaluate the various matching scales at their default values, namely $\mu_h = m_b$, $\mu_0 = \Delta$, and $\mu_i = \mu = \sqrt{m_b\Delta}$, where the values of Δ are different in the numerator and denominator. To study the residual scale dependence, we then vary each of the four scales by a factor of $\sqrt{2}$, correlated between numerator and denominator. While the ratio T is formally independent of these scales, the residual dependence of the truncated perturbative expression can be taken as an estimate of higher-order effects. The results are depicted in Fig. 1. Not surprisingly, the dominant effect arises from varying the lowest scale $\mu_0 \sim \Delta$, while the scale variations at the intermediate and high scales have a lesser impact.

The term proportional to $p_3(\Delta/m_b)$ in (3) includes a subset of power corrections associated with a phase-space factor. Whereas it was possible to perform the scale separation for these terms, treating them in a different way than the remaining power corrections in $\delta F(E_0)$ is somewhat arbitrary. The right plot in the figure refers to the form of the factorization formula shown in (3), whereas the left plot corresponds to expanding out $(p_3 - 1)$ in fixed-order perturbation theory and including it in the δF term. While the stability with respect to variations of the soft scale is better in this case, the perturbative corrections turn out to be
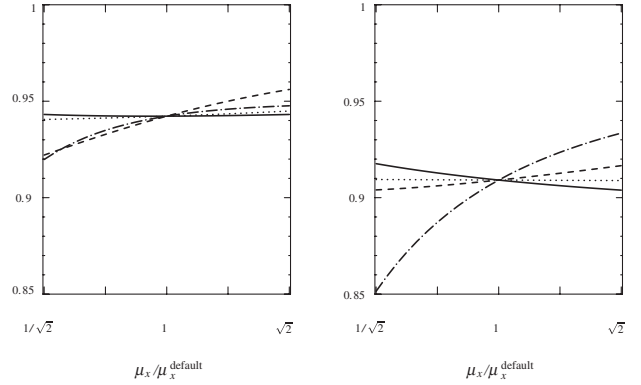

FIG. 1.   Scale dependence of the ratio T. The curves show the effect of varying the hard scale μ_h (dotted), intermediate scale μ_i (dashed), soft scale μ_0 (dash-dotted), and the reference scale μ (solid) by a factor of $\sqrt{2}$ about their default values. In the left plot the resummation is performed for the leading-power terms only, while in the right plot the p_3 term is also included (see text for further explanation).

smaller when performing the resummation for the p_3 term. The shift in central value between the two schemes is about 3%, which is inside the error bar. This effect hints at the importance of RG resummation for the power corrections.

To quote our final result we take the average of the two schemes and assign an asymmetric error reflecting the scale variation. This yields

$$T = 0.93^{+0.03}_{-0.05}\text{pert} \pm 0.02_{\text{hadr}} \pm 0.02_{\text{pars}}. \qquad (8)$$

The event fraction $F(E_0)$ receives hadronic power corrections not suppressed by inverse powers of m_b, but only by powers of the soft scale Δ [14]. These corrections are governed by B-meson matrix elements of local operators. The leading effect proportional to μ_π^2 in (3) is small mainly due to the smallness of its coefficient $\eta(1-\eta)/6$. Generically, we expect subleading corrections to scale like $\eta(\Lambda_{\text{QCD}}/\Delta)^3$, for which we assign a 2% uncertainty. The main uncertainties from parameter variations are $\mp0.9\%$ for $\alpha_s(m_Z) = 0.1189 \pm 0.0020$, $\pm0.4\%$ for $m_c/m_b = 0.26 \pm 0.03$, and $\pm0.1\%$ for $m_b = 4.61 \pm 0.06$ GeV. We also include a variation of $\pm1.2\%$ due to the fact that the three-loop anomalous dimension of the shape function is yet unknown [22]. Our value for the ratio T is lower than the estimate $T = 0.963$ obtained in fixed-order perturbation theory [8,9]. Moreover, we find that there is a significant theoretical uncertainty inherent in the calculation of T.

To complete the analysis we need as input the theoretical result for the $\bar{B} \to X_s\gamma$ branching fraction with $E_0 = 1.0$ GeV, which we take from the fixed-order NNLO calculation of [8,9]. These authors find $\mathcal{B}(\bar{B} \to X_s\gamma) = (3.27 \pm 0.23) \times 10^{-4}$ for $E_0 = 1$ GeV, where the error has been obtained by adding in quadrature the uncertainties from higher-order perturbative corrections (3%), nonperturbative effects (5%), parameter dependencies (3%), and

the interpolation in the charm-quark mass employed in the NNLO estimate of charm-penguin loop graphs (3%). The $\bar{B} \to X_s \gamma$ branching fraction receives incalculable power corrections starting at order $\Lambda_{\rm QCD}/m_b$, which cannot be described using the operator product expansion [26]. We agree with [8,9] on the assumption that the corresponding uncertainty should not exceed 5%. Recently, a new class of enhanced power corrections has been identified [17]. At tree level their effects are parametrized in terms of B-meson matrix elements of nonlocal four-quark operators. Using the vacuum insertion approximation, a reduction of the total branching fraction between 0.3% and 3% has been found. Accounting for this effect lowers the central value from 3.27 to 3.22.

Our final prediction for the $\bar{B} \to X_s \gamma$ branching fraction with $E_0 = 1.6$ GeV is

$$\mathcal{B}(\bar{B} \to X_s \gamma) = (2.98^{+0.13}_{-0.17}{}_{\rm pert} \pm 0.16_{\rm hadr} \pm 0.11_{\rm pars} \pm 0.09_{m_c})$$
$$\times 10^{-4}, \tag{9}$$

where we have combined errors of the same type in quadrature. This appears justified, because theoretical correlations in the calculations of the total branching fraction and the event fraction $F(E_0)$ are small. In (1) we have combined all uncertainties in quadrature. A more conservative approach would be to add the errors linearly, in which case the error becomes $^{+0.49}_{-0.53}$. Compared with the result $\mathcal{B}(\bar{B} \to X_s \gamma) = (3.15 \pm 0.23) \times 10^{-4}$ obtained in [8], our central value in (9) is lower by about 5% and, more importantly, the perturbative uncertainty is larger by almost a factor of 2. Both changes are a result of significant two-loop corrections encountered at the intermediate and soft scales, $\mu_i \sim \sqrt{m_b \Delta}$ and $\mu_0 \sim \Delta$.

Our theoretical prediction for the $\bar{B} \to X_s \gamma$ decay rate is consistent with the present experimental world average, as is reflected in the ratio

$$\frac{\mathcal{B}(\bar{B} \to X_s \gamma)_{\rm expt}}{\mathcal{B}(\bar{B} \to X_s \gamma)_{\rm th}} = 1.19 \pm 0.09_{\rm expt} \pm 0.10_{\rm th}. \tag{10}$$

However, whereas for a long time the experimental result used to be lower than the theoretical one, it is now about 1.4 standard deviations higher. Because in many extensions of the standard model the contributions from new physics are expected to interfere constructively with the standard model $b \to s \gamma$ amplitude, the situation has changed from one where new physics models were rather tightly constrained to one where there is now room for speculation about how the central number in (10) could be explained in terms of loop contributions containing new heavy particles. Consider, e.g., the case of type-II two-Higgs-doublet models. Whereas in the past there used to be bounds on the charged-Higgs mass from $\bar{B} \to X_s \gamma$ on the order of 500 GeV, the ratio (10) could now be explained with a new physics contribution from a charged Higgs in just that mass range.

In summary, we have presented a NNLO prediction for the $\bar{B} \to X_s \gamma$ branching fraction in which the effects of a photon-energy cut $E_\gamma \geq 1.6$ GeV have been properly taken into account. Low-scale perturbative corrections lower the prediction for the branching ratio and introduce a significant theoretical uncertainty even at NNLO. Our result is about 1.4 standard deviations lower than the world-average experimental value. This reopens the door for explorations of new physics contributions to rare flavor-changing B-decay processes.

[1] M. Misiak and M. Steinhauser, Nucl. Phys. **B683**, 277 (2004).
[2] M. Gorbahn and U. Haisch, Nucl. Phys. **B713**, 291 (2005).
[3] M. Gorbahn, U. Haisch, and M. Misiak, Phys. Rev. Lett. **95**, 102004 (2005).
[4] M. Czakon, U. Haisch, and M. Misiak (to be published).
[5] K. Bieri, C. Greub, and M. Steinhauser, Phys. Rev. D **67**, 114019 (2003).
[6] I. Blokland, A. Czarnecki, M. Misiak, M. Slusarczyk, and F. Tkachov, Phys. Rev. D **72**, 033014 (2005).
[7] H. M. Asatrian *et al.*, Nucl. Phys. **B749**, 325 (2006).
[8] M. Misiak and M. Steinhauser, hep-ph/0609241.
[9] M. Misiak *et al.*, hep-ph/0609232.
[10] O. L. Buchmüller and H. U. Flächer, Phys. Rev. D **73**, 073008 (2006).
[11] E. Barberio *et al.* (Heavy Flavor Averaging Group (HFAG)), hep-ex/0603003.
[12] K. Melnikov and A. Mitov, Phys. Lett. B **620**, 69 (2005).
[13] H. M. Asatrian *et al.*, hep-ph/0607316.
[14] M. Neubert, Eur. Phys. J. C **40**, 165 (2005).
[15] T. Becher and M. Neubert, Phys. Lett. B **633**, 739 (2006).
[16] T. Becher and M. Neubert, Phys. Lett. B **637**, 251 (2006).
[17] S. J. Lee, M. Neubert, and G. Paz, hep-ph/0609224.
[18] G. P. Korchemsky and G. Sterman, Phys. Lett. B **340**, 96 (1994).
[19] M. Neubert, Phys. Rev. D **49**, 3392 (1994); Phys. Rev. D **49**, 4623 (1994).
[20] T. Becher and M. Neubert, Phys. Rev. Lett. **97**, 082001 (2006).
[21] M. Neubert, Phys. Rev. D **72**, 074025 (2005).
[22] T. Becher and M. Neubert (to be published).
[23] Z. Ligeti, M. Luke, A. V. Manohar, and M. B. Wise, Phys. Rev. D **60**, 034019 (1999).
[24] S. W. Bosch, B. O. Lange, M. Neubert, and G. Paz, Nucl. Phys. **B699**, 335 (2004).
[25] M. Neubert, Phys. Lett. B **612**, 13 (2005).
[26] M. B. Voloshin, Phys. Lett. B **397**, 275 (1997).